

FINITE-DIFFERENCE SEMI-LAGRANGIAN TECHNIQUES FOR INTEGRATING  
THE SHALLOW WATER EQUATIONS ON THE SPHERE

J. R. Bates<sup>1</sup>

Laboratory for Atmospheres, NASA/Goddard Space Flight Center,  
Greenbelt, Maryland, USA

1. INTRODUCTION

Semi-Lagrangian techniques involve the integration of part or all of the equations of motion along particle trajectories, where the trajectories either arrive at or depart from a regular array of gridpoints. The impetus for the development of these techniques arises from the desire to avoid restrictive computational stability criteria, so that the integration time step can be chosen on the basis of accuracy considerations alone.

Since trajectory integration is the essence of the semi-Lagrangian technique, the time and spatial aspects of the discretization become intimately linked. Problems of devising appropriate numerical representations of the non-linear advection terms in an Eulerian scheme devolve to problems of estimating trajectories and of interpolating values of variables from/to gridpoints to/from trajectory end points in a semi-Lagrangian scheme. The possibility of unconditional stability in a semi-Lagrangian scheme arises when the scheme is constructed in such a way as to ensure that the domain of numerical dependence always surrounds the trajectories.

In the first two decades of NWP, some effort was devoted to the development of semi-Lagrangian schemes: see Haltiner (1971) for a discussion. Interest gradually declined, however, to the point where these schemes received no mention in the second edition of the above textbook (Haltiner and Williams, 1980). The recent resurgence of interest was initiated by the work of Robert (1981, 1982), who showed that a multiply-upstream form of the semi-Lagrangian technique could be combined with the semi-implicit technique to give a scheme which allows stable integration of the shallow water equations with very long time steps. An analysis of

---

<sup>1</sup> On leave of absence from the Irish Meteorological Service, Dublin

the semi-Lagrangian technique, showing why it was necessary to go multiply upstream to achieve unconditional stability, was given by Bates and McDonald (1982), and the technique was used to integrate a split multi-level PE model. (For further analysis, see McDonald, 1984, 1987). Subsequently, a variety of semi-Lagrangian schemes for integrating the shallow water equations have been proposed (Bates, 1984; Staniforth and Temperton, 1986; Ritchie, 1986; McGregor, 1987; Temperton and Staniforth, 1987) and a number of multi-level PE models have been developed (Robert *et al.*, 1985; McDonald, 1986; Bates and McDonald, 1987). All these models allow the use of long time steps.

The models developed by Robert and his co-workers have until recently used three time levels, while those developed by Bates and McDonald have used two time levels. McGregor has also adopted the two-time-level approach. Two-time-level schemes have the following advantages vis-a-vis three-time-level schemes: (1) they are potentially much more efficient, (2) they have no computational mode, (3) they have smaller storage requirements, (4) they are easier to code. The main disadvantage of two-time-level schemes is the absence of velocity components at the middle time level for estimating trajectories. This disadvantage can be minimized, however, by storing the velocities from previous time levels and doing an extrapolation in time to give estimates of the time-centered velocities (see McDonald and Bates, 1987; Temperton and Staniforth, 1987).

All the papers referred to above have used a limited area as the domain of integration. There is a natural interest in extending semi-Lagrangian schemes to the global domain. One of the problems associated with limited area models - that particles may originate outside the domain of integration - no longer occurs when a model becomes global. It is therefore possible that semi-Lagrangian schemes will only achieve their full potential in the global context. Before this can occur, however, the problems associated with the polar singularity in the latitude - longitude coordinate system must be solved. From the point of view of semi-Lagrangian integration, these are the following:

- 1) The departure point corresponding to a near-polar gridpoint cannot be accurately located by going back along the coordinate lines using the known velocity components at a single point, because of the strong curvature of the coordinate lines near the singularity.
- 2) The momentum equations in component form cannot be accurately integrated along a near-polar trajectory corresponding to a long time step, because of the rapid spatial variation of all terms in the equations (particularly

the curvature terms) along such a trajectory.

These problems can be overcome by introducing, for use in conjunction with the spherical system, an auxiliary coordinate system which does not have a singularity at the poles. Possible auxiliary systems which can be used are the following:

- a) North and south polar stereographic projections.
- b) A Cartesian coordinate system whose origin is at the centre of the earth (Ritchie, 1987).
- c) A rotated spherical coordinate system at each near-polar gridpoint, whose equator passes through the gridpoint in question (McDonald and Bates, 1988).

An alternative method of overcoming Problem 2 is proposed in Section 3 below; it consists of integrating the momentum equation in vector form. The auxiliary system need then be used only in connection with Problem 1.

## 2. A GLOBAL SEMI-LAGRANGIAN SHALLOW WATER MODEL

In this section the global semi-Lagrangian shallow water model of McDonald and Bates (1988) is described and some results of integrations are presented. The numerical scheme is based on the two-step semi-implicit method of McDonald (1986) and uses a spherical C-grid (see Fig. 1) with two time levels. An auxiliary spherical coordinate system is used at each near-polar gridpoint of the original latitude-longitude grid. The auxiliary system is obtained by a rotation such that the new equator passes through the gridpoint in question and the new coordinate directions coincide with those of the original system at that point (see Fig. 2). The departure points are located and the momentum equations integrated in the auxiliary system at the near-polar gridpoints.

The governing equations are the shallow water equations with divergence damping included, i.e.,

$$\frac{d_H u}{dt} = - \frac{1}{a \cos \theta} \frac{\partial}{\partial \lambda} (\phi - cD) + fv + C_u \quad (1)$$

$$\frac{d_H v}{dt} = - \frac{1}{a} \frac{\partial}{\partial \theta} (\phi - cD) - fu + C_v \quad (2)$$

$$\frac{d_H \phi}{dt} = - \phi D \quad (3)$$

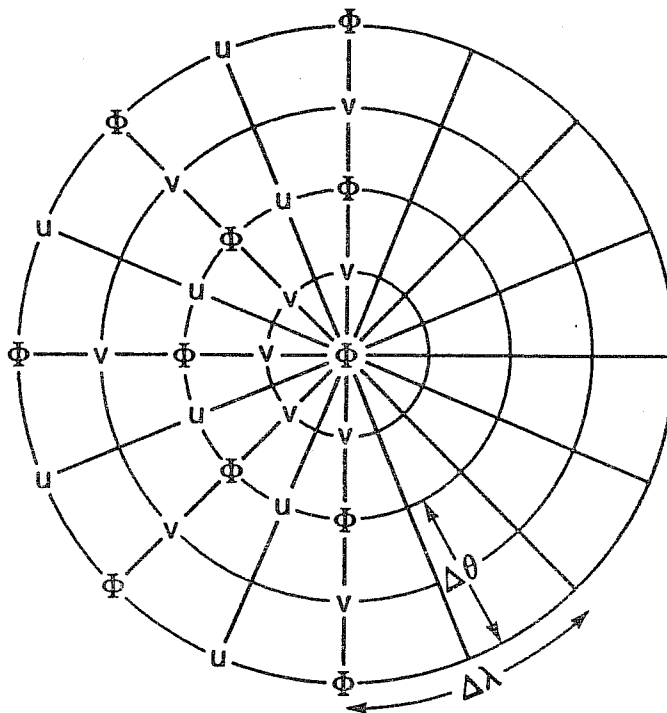


Fig. 1. The distribution of points on the C-grid in the neighborhood of the pole.

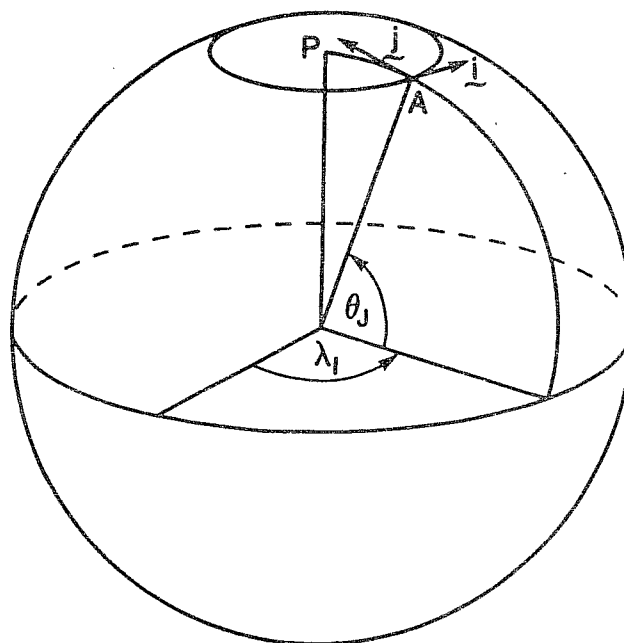


Fig. 2. The auxiliary coordinate system at point A is obtained by rotating the geographical spherical system through the angles  $\lambda_I$  and  $\theta_J$ .

where  $d_H/dt$  is the horizontal Lagrangian derivative,  $D$  is the divergence,  $c$  is the coefficient of divergence damping and  $(C_u, C_v)$  are the curvature terms. We use two methods of integrating these equations, the first applying in regions removed from the poles, the second in regions near the poles.

(a) Regions removed from the poles ( $|\theta| \leq \theta_M$ )

Here the departure points are located and the momentum equations integrated in the geographical spherical coordinate system. The estimate of the departure point corresponding to the arrival point  $(\lambda, \theta)$  is given by

$$\lambda_* = \lambda - \left( \frac{\hat{u}}{a \cos \theta} \right) \Delta t \quad (4)$$

$$\theta_* = \theta - \left( \frac{\hat{v}}{a} \right) \Delta t \quad (5)$$

where  $(\hat{u}, \hat{v})$  are the time and space-centered estimates of the velocity components along the trajectory (see McDonald and Bates, 1987).

The momentum equations are integrated in two half steps of  $\Delta t/2$  as in McDonald (1986), the Coriolis and pressure gradient terms alternately being treated implicitly:

Step 1

$$(u^{n+1/2} - u_*^n) / (\Delta t/2) = \left[ -\frac{1}{a \cos \theta} \frac{\partial}{\partial \lambda} (\phi - cD) + 2 C_u \right]_*^n + f_* v^{n+1/2} \quad (6)$$

$$(v^{n+1/2} - v_*^n) / (\Delta t/2) = \left[ -\frac{1}{a} \frac{\partial}{\partial \theta} (\phi - cD) + 2 C_v \right]_*^n - f_* u^{n+1/2} \quad (7)$$

Step 2

$$(u^{n+1} - u^{n+1/2}) / (\Delta t/2) = \left[ -\frac{1}{a \cos \theta} \frac{\partial}{\partial \lambda} (\phi - cD) \right]_*^{n+1} + f_* v^{n+1/2} \quad (8)$$

$$(v^{n+1} - v^{n+1/2}) / (\Delta t/2) = \left[ -\frac{1}{a} \frac{\partial}{\partial \theta} (\phi - cD) \right]_*^{n+1} - f_* u^{n+1/2} \quad (9)$$

The continuity equation is integrated in a single step  $\Delta t$  as follows:

$$(\phi^{n+1} - \phi_*^n)/\Delta t = -(\bar{\phi}/2)[D^{n+1} + D_*^n] - (\phi'D)_*^n \quad (10)$$

In the above,  $\bar{\phi}$  is a constant such that  $\phi = \bar{\phi} + \phi'$ ,  $|\phi'| \ll \bar{\phi}$ . Variables without subscripts denote values at an arrival point while variables with a star subscript denote values at the corresponding departure point.

We solve (6,7) for  $(u,v)^{n+1/2}$  and eliminate these quantities from (8,9). Bringing all  $(n+1)$  level quantities to the l.h.s., equations (8,9, 10) then give

$$[u + \frac{\Delta t}{2} \frac{1}{a \cos \theta} \frac{\partial}{\partial \lambda} (\phi - cD)]^{n+1} = (B_u)_*^n \quad (11)$$

$$[v + \frac{\Delta t}{2} \frac{1}{a} \frac{\partial}{\partial \theta} (\phi - cD)]^{n+1} = (B_v)_*^n \quad (12)$$

$$[\phi + \frac{\Delta t}{2} \bar{\phi} D]^{n+1} = (B_\phi)_*^n \quad (13)$$

where the right hand sides involve known quantities interpolated to the departure points from surrounding grid points. Eliminating the velocity components  $(u,v)^{n+1}$ , the above equations reduce to a Helmholtz equation in  $\phi^{n+1}$ :

$$\nabla^2 \phi^{n+1} - \mu^2 \phi^{n+1} = H \quad (14)$$

where  $\mu^2$  is a constant and H is a known forcing function.

(b) Regions near the poles ( $|\theta| > \theta_M$ )

In the neighborhood of the poles we continue to integrate our equations using the gridpoints of the original  $(\lambda, \theta)$  C-grid (See Fig. 1). However, for the purposes of accurately locating the departure points and of integrating the momentum equations in a system in which their terms are smoothly varying, we introduce for each near-polar gridpoint A (at which  $\lambda = \lambda_I$ ,  $\theta = \theta_j$ ) an auxiliary spherical coordinate system  $(\lambda', \theta')$  such that in the new coordinate system the point A lies at  $(\lambda' = 0, \theta' = 0)$  and the coordinate unit vectors  $(\underline{i}, \underline{j})$  at point A in both systems coincide (see Fig. 2).

Due to the small curvature of the coordinate lines in the auxiliary system in the neighborhood of point A, the departure point corresponding to point A can be accurately located using the formulae

$$\lambda_*^1 = - \left( \frac{\hat{u}'}{a \cos \theta'} \right) \Delta t \quad (15)$$

$$\theta_*' = - \left( \frac{\hat{v}'}{a} \right) \Delta t \quad (16)$$

where  $(\hat{u}', \hat{v}')$  are time and space-centered estimates of the velocity components along the trajectory in the auxiliary system. These are obtained by interpolating the velocity components in the original system to the midpoint of the trajectory and using the spherical transformation formulae

$$u' = \mathcal{L}u - \mathcal{S}v \quad (17)$$

$$v' = \mathcal{S}u + \mathcal{L}v \quad (18)$$

where

$$\mathcal{L} = [\cos\theta\cos\theta_J + \sin\theta\sin\theta_J\cos(\lambda - \lambda_I)]/\cos\theta'$$

$$\mathcal{S} = \sin\theta_J\sin(\lambda - \lambda_I)/\cos\theta'$$

Note that at point A,  $\mathcal{L} = 1$ ,  $\mathcal{S} = 0$ . The coordinates in the  $(\lambda, \theta)$  system of the departure point given by (15), (16) are evaluated using the inverse transformation formulae

$$\lambda = \lambda_I + \tan^{-1} \left[ \frac{\cos\theta'\sin\lambda'}{\cos\theta'\cos\lambda'\cos\theta_J - \sin\theta'\sin\theta_J} \right]$$

$$\theta = \sin^{-1} [\cos\theta'\cos\lambda'\sin\theta_J + \sin\theta'\sin\theta_J]$$

To determine the departure points for the poles themselves, which are needed in integrating the continuity equation, we use the first Fourier component of the time-centered meridional velocity components lying at the points  $\Delta\theta/2$  away from the poles.

The momentum equations are integrated in the auxiliary system using the same scheme as described in section (a) for the original system. This leads to an equation in the auxiliary system identical in form to (11, 12). Since the arrival point lies on the equator in the auxiliary system, the curvature terms are negligible. Omitting them and using the formulae (17, 18) to transform the time-differenced form of the momentum equations back to the original system we obtain

$$\left[ u + \frac{\Delta t}{2} \frac{1}{a\cos\theta} \frac{\partial}{\partial t} (\phi - cD) \right]^{n+1} = A_u \quad (19)$$

$$\left[ v + \frac{\Delta t}{2} \frac{1}{a} \frac{\partial}{\partial \theta} (\phi - cD) \right]^{n+1} = A_v \quad (20)$$

where

$$A_u = \mathcal{L}^*(B_u)^n - \mathcal{S}^*(B_v)^n$$

$$A_v = \mathcal{S}^*(B_u)^n + \mathcal{L}^*(B_v)^n$$

Here the  $(B_u, B_v)$  are of the same form as in section (a), apart from the omitted curvature terms.

The continuity equation, which involves only scalars, maintains the same form (13) as before, and when (19, 20) are used to eliminate the divergence we again obtain an equation of the form (14) for  $\phi^{n+1}$ , the only difference being a modified form of the forcing function H. Thus, our auxiliary system has allowed an extension of the Helmholtz equation to the whole sphere, while overcoming the problems associated with the polar singularity. The Helmholtz equation is solved using the fast solver of Sweet (1977).

In all our numerical computations we used bicubic interpolation to obtain values at departure points, while using bilinear interpolation to obtain values at the mid-points of trajectories for the purpose of space centering. In the case of points lying in the immediate neighborhood of the poles, the interpolations used values at gridpoints lying on the other side of the poles. Whenever vector components from across the poles were used, they underwent a change of sign. All divergences at the poles were evaluated using the integral rather than the differential definition of the divergence.

Numerical integrations were carried out to test the proposed scheme on the spherical domain. As initial state we took a geopotential field given by

$$\phi(\lambda, \theta, 0) = \bar{\phi} + 2\Omega a v_0 \sin^3 \theta \cos \theta \sin \lambda \quad (21)$$

where  $\Omega$  and  $a$  are respectively, the earth's rotation rate and radius. The initial wind field was derived from (21) using the geostrophic relationship. Thus, the initial cross-polar flow was of strength  $v_0$ , while both wind components were zero at the equator. The values  $\bar{\phi} = 5.77 \times 10^4 \text{ m}^2/\text{s}^2$  and  $v_0 = 20 \text{ m/s}$  were used in the integrations. The initial fields are displayed in Fig. 3.

The model was integrated with  $\Delta\lambda = 2^\circ$ ,  $\Delta\theta = 4.5^\circ$ ,  $\Delta t = 1.5\text{h}$ ,



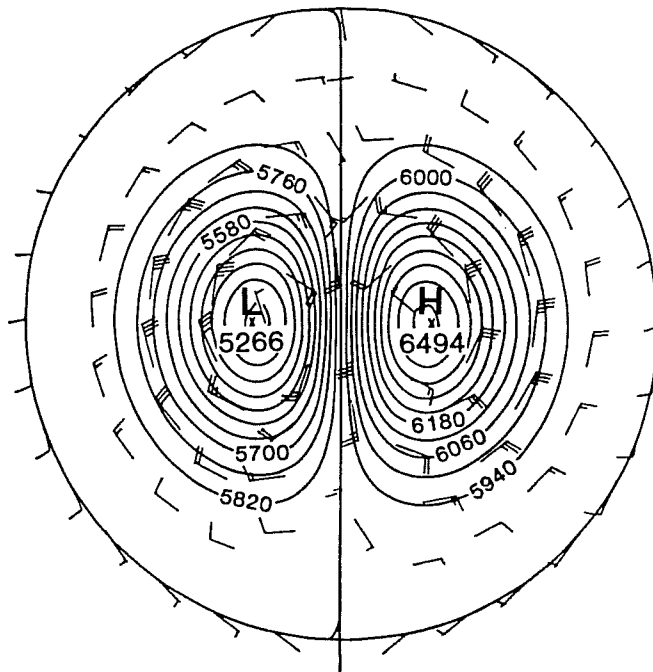


Fig. 3. The initial field (geopotential height in metres, wind in knots) in the northern hemisphere.

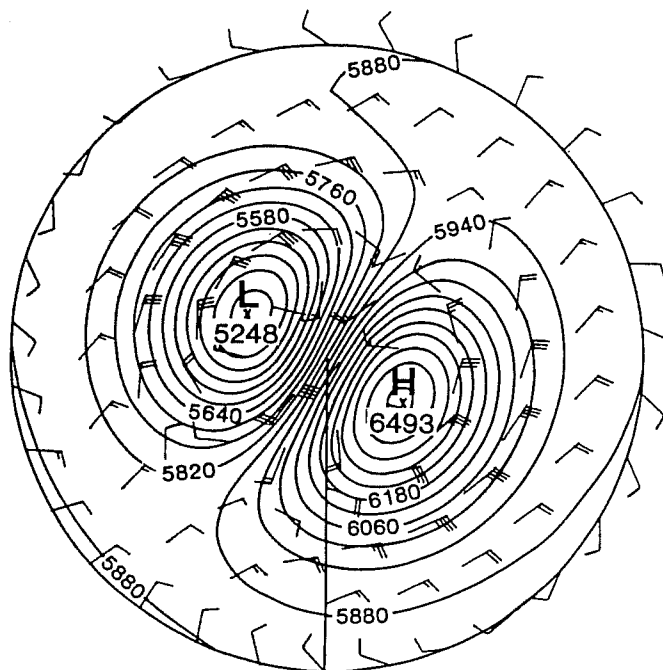


Fig. 4. Results of 1 day integration.

$\theta_M = 70^\circ$ ,  $c = 0$ . The results at 1 day and 5 days are shown in Figs. 4 and 5. It can be seen that there are no signs of instability. The true solution is unknown, but the results shown are very close to those obtained with  $\Delta t$  reduced to 10 min, leaving all other parameters unchanged. Though the integration scheme does not formally conserve mass, the mass loss over the 5 day period with  $\Delta t = 1.5$  h amounted to only  $4.68 \times 10^{-3}\%$ .

As a test, the model was integrated for a 30 day period. Over this period, problems did occur. Appreciable mass losses and unmeteorological flow situations were encountered. These problems were found to be alleviated by introducing divergence damping and by decreasing the value of  $\theta_M$ . Work is in progress to try to further alleviate the the problems found with the two-step SLSI scheme.

### 3. FURTHER DEVELOPMENTS

To date, the work of Bates and McDonald on semi-Lagrangian schemes has been directed towards discretizing the governing equations in such a way that the eventual equations to be solved are both simple and amenable to very efficient numerical solution. Thus, the semi-Lagrangian and alternating direction implicit (SLADI) scheme (Bates, 1984; Bates and McDonald, 1987) has led to a simple tridiagonal system of equations to be solved, while the two-step semi-Lagrangian and semi-implicit (SLSI) scheme (McDonald, 1986; McDonald and Bates, 1988) has led to a simple Helmholtz equation.

A price has been paid for the simplicity achieved, however, in that both these schemes involve truncation errors over and above those which a straightforward centered-on-the-trajectory scheme would entail. A linear analysis of the two-time-level centered scheme, showing the truncation errors of the SLADI scheme relative to it, has been given by Bates (1984). The centered scheme is accurate and unconditionally stable. Its disadvantage is that it leads to a more complicated form of elliptic equation to be solved than either the SLADI or the two-step SLSI scheme.

The additional truncation errors of the uncentered schemes may not be significant for moderately long time steps or for short term integrations. For very long time steps or for longer term integrations, however, it seems desirable to minimize the truncation error, even if so doing results in a more complicated elliptic equation. When computer memory is not a constraint, achieving the simplest type of elliptic equation becomes less important, as direct solvers or multi-grid methods for solving more

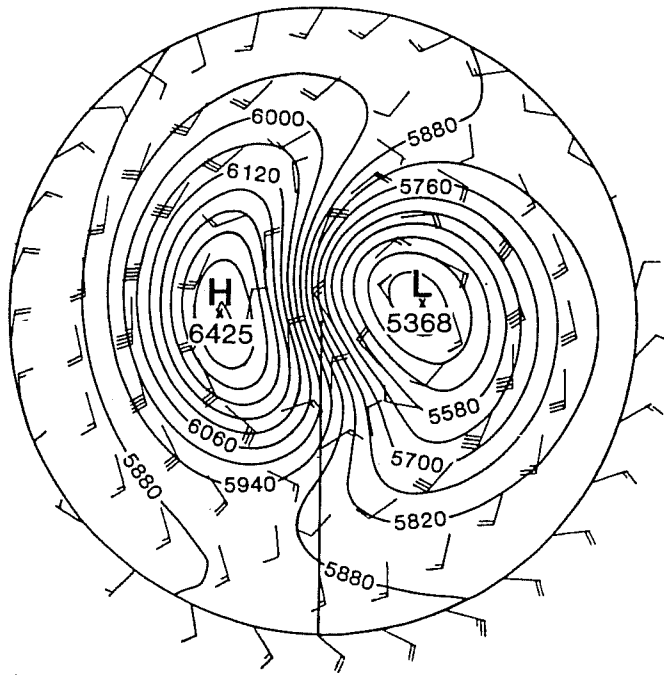


Fig. 5. Results of 5 day integration.

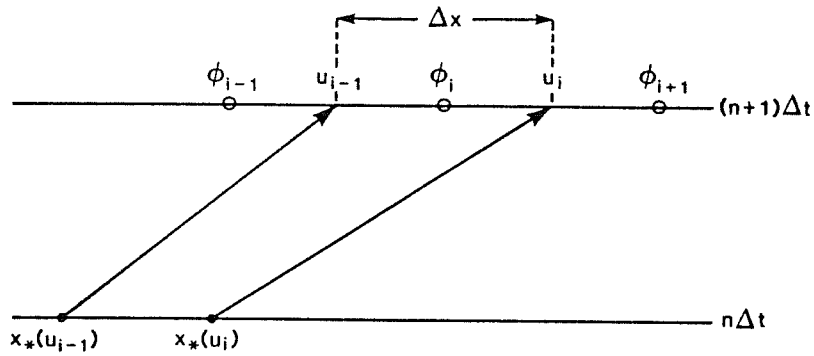


Fig. 6. The trajectories used for the mean mass element.

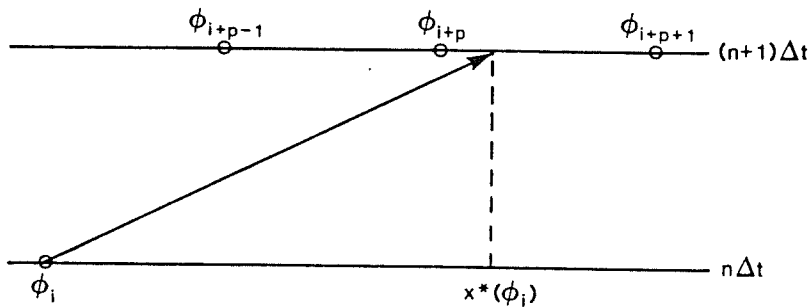


Fig. 7. The trajectory used for the perturbation mass element.

general types of elliptic equations may be used to advantage.<sup>2</sup>

Temperton and Staniforth (1987) have recently presented some impressive results obtained using an integration scheme which comes very close to being trajectory-centered in the full non-linear sense. The metric terms in the momentum equations are expressed at the estimated midpoint of the trajectory using a time extrapolation combination with an iterative space centering procedure. The continuity equation is expressed in logarithmic form, thus eliminating a source of non-linear uncenteredness which would otherwise occur.

Here, a scheme is presented which goes a stage further than that of Temperton and Staniforth; it achieves complete centeredness (without iteration) on the sphere by integrating the momentum equation in vector form and the continuity equation in fully Lagrangian form. In addition, the method of discretizing the continuity equation formally guarantees the conservation of mass over the global domain.

(a) Integration of the momentum equation in vector form

The momentum equation can be written in vector form as

$$\frac{d \underline{V}_{H-H}}{dt} = - \nabla(\phi - cD) - f \underline{k} \times \underline{V}_H \quad (22)$$

where  $\underline{V}_H$  is the horizontal wind vector and  $\underline{k}$  is the vertical unit vector. Unlike equations (1) and (2), all terms in (22) are smoothly varying near the poles as long as the physical quantities themselves are smoothly varying. We can therefore obtain an accurate integration of (22) by discretizing it as follows:

$$\begin{aligned} [(\underline{V}_H)^{n+1} - (\underline{V}_H)_*^n] / \Delta t = & - \frac{1}{2} [ \{ \nabla(\phi - cD) \}^{n+1} + \{ \nabla(\phi - cD) \}_*^n ] \\ & - \frac{1}{2} [ (f \underline{k} \times \underline{V}_H)^{n+1} + (f \underline{k} \times \underline{V}_H)_*^n ] \end{aligned}$$

i.e.

$$[\underline{V}_H + F \underline{k} \times \underline{V}_H + \frac{\Delta t}{2} \nabla(\phi - cD)]^{n+1} = [\underline{V}_H - F \underline{k} \times \underline{V}_H - \frac{\Delta t}{2} \nabla(\phi - cD)]_*^n \quad (23)$$

where  $F = f \Delta t / 2$ .

Having performed the trajectory integration in vector form, we now resolve into components. Eq. (23) can be written

$$\begin{aligned} & [u - Fv + \frac{\Delta t}{2} \frac{1}{a \cos \theta} \frac{\partial}{\partial \lambda} (\phi - cD)]^{n+1} \underline{i} + [v + Fu + \frac{\Delta t}{2} \frac{1}{a} \frac{\partial}{\partial \theta} (\phi - cD)]^{n+1} \underline{j} \\ & = [u + Fv - \frac{\Delta t}{2} \frac{1}{a \cos \theta} \frac{\partial}{\partial \lambda} (\phi - cD)]_*^n \underline{i}_* + [v - Fu - \frac{\Delta t}{2} \frac{1}{a} \frac{\partial}{\partial \theta} (\phi - cD)]_*^n \underline{j}_* \end{aligned} \quad (24)$$

where  $(\underline{i}_*, \underline{j}_*)$  are the unit vectors at the departure point. These are related to  $(\underline{i}, \underline{j})$ , the unit vectors at the arrival point, by the following formulae:

$$\underline{i}_* = \underline{i} \cos(\lambda - \lambda_*) - (\underline{j} \sin \theta - \underline{k} \cos \theta) \sin(\lambda - \lambda_*) \quad (25)$$

$$\begin{aligned} \underline{j}_* & = \underline{i} \sin \theta_* \sin(\lambda - \lambda_*) + \underline{j} [\cos \theta \cos \theta_* + \sin \theta \sin \theta_* \cos(\lambda - \lambda_*)] \\ & + \underline{k} [\sin \theta \cos \theta_* - \cos \theta \sin \theta_* \cos(\lambda - \lambda_*)] \end{aligned} \quad (26)$$

Substituting (25) and (26) into (24) and omitting the factors multiplying  $\underline{k}$  [this is consonant with the "traditional approximation" (Phillips, 1966) used in deriving the primitive equations], we equate the coefficients of  $(\underline{i}, \underline{j})$  to obtain

$$[u - Fv + \frac{\Delta t}{2} \frac{1}{a \cos \theta} \frac{\partial}{\partial \lambda} (\phi - cD)]^{n+1} = A_u \quad (27)$$

$$[v + Fu + \frac{\Delta t}{2} \frac{1}{a} \frac{\partial}{\partial \theta} (\phi - cD)]^{n+1} = A_v \quad (28)$$

where

$$A_u = (B_1)_*^n \sin \lambda + (B_2)_*^n \cos \lambda$$

$$A_v = (Y_v \cos \theta)_*^n \cos \theta + [(B_1)_*^n \cos \lambda - (B_2)_*^n \sin \lambda] \sin \theta$$

with

$$B_1 = Y_u \sin \lambda + Y_v \cos \lambda \sin \theta$$

$$B_2 = Y_u \cos \lambda - Y_v \sin \theta \sin \lambda$$

$$Y_u = u + Fv - \frac{\Delta t}{2} \frac{1}{a \cos \theta} \frac{\partial}{\partial \lambda} (\phi - cD)$$

$$Y_v = v - Fu - \frac{\Delta t}{2} \frac{1}{a} \frac{\partial}{\partial \theta} (\phi - cD)$$

Note that the curvature terms, which arise from the variation of  $\underline{i}$  and  $\underline{j}$ , have been implicitly taken into account in a completely centered manner by integrating the vector momentum equation along the trajectory.

Solving (27), (28) for  $(u, v)^{n+1}$  we obtain

$$u^{n+1} = \frac{1}{1+F^2} \left[ -\frac{\Delta t}{2} \left( \frac{1}{a \cos \theta} \frac{\partial}{\partial \lambda} + \frac{F}{a} \frac{\partial}{\partial \theta} \right) (\phi - cD)^{n+1} + (A_u + FA_v) \right] \quad (29)$$

$$v^{n+1} = \frac{1}{1+F^2} \left[ \frac{\Delta t}{2} \left( \frac{F}{a \cos \theta} \frac{\partial}{\partial \lambda} - \frac{1}{a} \frac{\partial}{\partial \theta} \right) (\phi - cD)^{n+1} + (A_v - FA_u) \right] \quad (30)$$

whence we have

$$D^{n+1} = -\frac{\Delta t}{2} \left( \frac{1}{1+F^2} \right) \left[ V^2 - \frac{C_1(\theta)}{a \cos \theta} \frac{\partial}{\partial \lambda} - \frac{C_2(\theta)}{a} \frac{\partial}{\partial \theta} \right] (\phi - cD)^{n+1} + A \quad (31)$$

where A is a known quantity and

$$C_1(\theta) = \frac{1-F^2}{1+F^2} \frac{1}{a} \frac{\partial F}{\partial \theta}$$

$$C_2(\theta) = \frac{2F}{1+F^2} \frac{1}{a} \frac{\partial F}{\partial \theta}$$

#### (b) A mass conserving discretization of the continuity equation

The principle of mass conservation following a fluid element can be written in fully Lagrangian form as follows:

$$\frac{d}{dt} (\delta M) = 0 \quad (32)$$

where  $\delta M$  is the mass of the fluid element. [For a discussion of the Eulerian and Lagrangian forms of the continuity equation, see Holton (1979), Chapter 2].

A discretization of the above equation is now presented which conserves mass over the global domain, which maintains the property of unconditional stability (in a linear tangent plane analysis) when coupled with (27) and (28), and which leads to an elliptic equation for  $\phi^{n+1}$ . The absence of any terms on the r.h.s. of (32) eliminates a source of non-linear uncenteredness such as is associated with the r.h.s. of (3). Integrating (32) along a trajectory we obtain

$$(\delta M)_i^{n+1} = (\delta M)_*^n \quad (33)$$

In order to present the mass-conserving scheme in as clear a manner as possible, we confine our attention in the first instance to the case of the shallow water equations in one dimension. Adopting a staggered grid (see Fig. 6) where the coordinates of the  $\phi_i$  and  $u_i$  gridpoints are given by  $i\Delta x$  and  $(i+1/2)\Delta x$ , respectively, we identify  $(\delta M)_i^{n+1}$  as the mass element centered on the  $\phi_i$  gridpoint at time  $(n+1)\Delta t$ , i.e.

$$(\delta M)_i^{n+1} = \phi_i^{n+1} \Delta x \quad (34)$$

We separate the r.h.s. of (33) into mean and perturbation parts, where the mean part is associated with  $\bar{\phi}$  and the perturbation part with  $\phi'$ . Thus (33) can be written

$$\phi_i^{n+1} \Delta x = (\delta \bar{M})_{*i}^n + (\delta M')_{*i}^n \quad (35)$$

Here we have added the subscript  $i$  on the r.h.s. to indicate that both quantities are associated with the  $\phi_i$  gridpoint. In order to arrive at a scheme which is both stable and mass conserving, we adopt different methods of treating the mean and perturbation parts.

The mean part is defined as the mean mass contained at time  $n\Delta t$  between the trajectories which arrive at the  $u_i$  and  $u_{i-1}$  gridpoints at time  $(n+1)\Delta t$  (see Fig. 6); thus,

$$(\delta \bar{M})_{*i}^n = \bar{\phi} [x_*(u_i) - x_*(u_{i-1})] \quad (36)$$

where  $x_*(u_i)$  is the coordinate of the departure point of the trajectory arriving at the  $u_i$  gridpoint. To evaluate  $x_*(u_i)$  we formally integrate the equation

$$\frac{dx}{dt} = u$$

in a centered manner to give

$$x_*(u_i) = (i + 1/2)\Delta x - \frac{\Delta t}{2}[u_i^{n+1} + u_{*i}^n] \quad (37)$$

where  $u_{*i}^n$  is an estimate of the velocity at  $x_*(u_i)$  at time  $n\Delta t$ . using this, (36) gives

$$(\delta \bar{M})_{*i}^n = \bar{\phi} \Delta x \left[ 1 - \frac{\Delta t}{2} \{ (\delta_x u)_i^{n+1} + (\delta_x u_*)_i^n \} \right] \quad (38)$$

where

$$(\delta_x u)_i^{n+1} = [u_i^{n+1} - u_{i-1}^{n+1}] / \Delta x$$

$$(\delta_x u_*)_i^n = [u_{*i}^n - u_{*i-1}^n] / \Delta x$$

Assuming the domain is periodic, it follows from (38) that

$$\sum_{i=1}^N (\delta \bar{M})_{*i}^n = \bar{\phi} L \quad (39)$$

where  $N$  is the number of grid intervals and  $L = N \Delta x$ . Thus, mean mass is conserved over the domain.

The perturbation part is defined, by contrast, in terms of trajectories which depart from gridpoints at the old time level. Let the trajectory which departs from the  $\phi_i$  gridpoint at time  $n \Delta t$  arrive at  $x^*(\phi_i)$  at time  $(n+1) \Delta t$  (see Fig. 7). We associate the perturbation mass element  $(\phi')_i^n \Delta x$  with this trajectory and distribute this element to a number of  $\phi$ -gridpoints surrounding  $x^*(\phi_i)$  at the new time level. Any number of points can be chosen for the distribution, with appropriate weights assigned to each point. Consider, for instance, the case where three points are chosen; if  $\phi_{i+p}$  is the nearest  $\phi$ -point to  $x^*(\phi_i)$ , our three points will be the  $(\phi_{i+p-1}, \phi_{i+p}, \phi_{i+p+1})$  gridpoints. Defining

$$\hat{\alpha}_i = [x^*(\phi_i) - (i+p)\Delta x] / \Delta x$$

we distribute the perturbation mass element  $(\phi')_i^n \Delta x$  to these three points with weights  $(w_1, w_2, w_3)$ , respectively, where

$$w_1 = -\frac{\hat{\alpha}_i(1-\hat{\alpha}_i)}{2}$$

$$w_2 = (1-\hat{\alpha}_i)(1+\hat{\alpha}_i)$$

$$w_3 = \frac{\hat{\alpha}_i(1+\hat{\alpha}_i)}{2}$$

We see that

$$w_1 + w_2 + w_3 = 1$$



so none of the perturbation mass gets lost. The same procedure is applied to the trajectories starting from all  $\phi_i$  -points at time  $n\Delta t$ ; thus, the perturbation mass  $(\delta M')_{*i}^n$  received by the  $\phi_i$  gridpoint at time  $(n+1)\Delta t$  will, in general, consist of portions received from a number of adjacent trajectories.

The above procedure is, by definition, such as to conserve the perturbation mass globally. When it is combined with the mean mass updating procedure, it is clear that total mass is conserved. In the case of constant wind, the procedure can be shown to reduce to the formula for pure advection using quadratic interpolation, as analysed by Bates and McDonald (1982).

Using (38), we can write (35) in the form

$$[\phi + \bar{\phi} \frac{\Delta t}{2} \delta_x u]_{i}^{n+1} = \bar{\phi} [1 - \frac{\Delta t}{2} (\delta_x u)_{i}^n] + \frac{1}{\Delta x} (\delta M')_{*i}^n \quad (40)$$

This can be generalized to the two dimensional case on the sphere to give

$$[\phi + \bar{\phi} \frac{\Delta t}{2} D]_{i,j}^{n+1} = \bar{\phi} [1 - \frac{\Delta t}{2} (\nabla \cdot \underline{V})_{i,j}^n] + \frac{1}{\Delta s} (\delta M')_{*i,j}^n \quad (41)$$

where  $\Delta s$  is the element of area associated with the  $\phi_{i,j}$  gridpoint, and  $(\delta M')_{*i,j}^n$  is obtained by advecting and distributing perturbation mass elements in a manner analogous to the one-dimensional case described above. We see that the l.h.s. of (41) is identical to that of (13).

We now use (41) to eliminate  $D^{n+1}$  from the r.h.s. of (31) to give

$$D^{n+1} = - \frac{1}{C_3(\theta) \bar{\phi} \frac{\Delta t}{2}} \left[ \nabla^2 - \frac{C_1(\theta)}{a \cos \theta} \frac{\partial}{\partial \lambda} - \frac{C_2(\theta)}{a} \frac{\partial}{\partial \theta} \right] \phi^{n+1} + B \quad (42)$$

where

$$C_3(\theta) = \frac{1+F^2}{\bar{\phi} \frac{\Delta t^2}{4} + c \frac{\Delta t}{2}}$$

and  $B$  is a known quantity. Then using (42) to eliminate  $D^{n+1}$  from (41) we get the following elliptic equation for  $\phi^{n+1}$ :

$$\left[ \nabla^2 - \frac{C_1(\theta)}{a \cos \theta} \frac{\partial}{\partial \lambda} - \frac{C_2(\theta)}{a} \frac{\partial}{\partial \theta} - C_3(\theta) \right] \phi^{n+1} = \hat{H} \quad (43)$$

where  $\hat{A}$  is a known forcing function. We note that, as in the case of the two-step SLSI scheme, the inclusion of an implicit divergence damper has not altered the form of the elliptic equation.

Once (43) is solved for  $\phi^{n+1}$ , equation (41) gives  $D^{n+1}$  and equation (29) and (30) give  $(u, v)^{n+1}$ , thus completing the solution.

If we linearize equations (27), (28) and (41) on a tangent plane, we obtain the set of centered equations analysed by Bates (1984), Section 4a, which were shown to give unconditional stability.

A global semi-Lagrangian model based on the above ideas is at present being developed at NASA/GLA. Results will be reported as soon as they are available.

#### References

Bates, J. R., 1984: An efficient semi-Lagrangian and alternating direction implicit method for integrating the shallow water equations. Mon. Wea. Rev., 112, 2033-2047.

Bates, J. R., and A. McDonald, 1982: Multiply-upstream, semi-Lagrangian advective schemes: analysis and application to a multilevel primitive equation model. Mon. Wea. Rev., 110, 1831-1842.

\_\_\_\_\_, 1987: A semi-Lagrangian and alternating direction implicit method for integrating a multilevel primitive equation model. J. Met. Soc. Japan, (in press).

Haltiner, G. J., 1971: Numerical Weather Prediction. John Wiley and Sons, 317 pp.

\_\_\_\_\_, and R. T. Williams, 1980: Numerical Prediction and Dynamic Meteorology (Second Edition). John Wiley L. Sons, 477 pp.

Holton, J. R., 1979: An Introduction to Dynamic Meteorology (Second Edition) Academic Press, 391 pp.

- McDonald, A., 1984: Accuracy of multiple-upstream, semi-Lagrangian advective schemes. Mon. Wea. Rev., 112, 1267-1275.
- \_\_\_\_\_, 1986: A semi-Lagrangian and semi-implicit two time-level integration scheme. Mon. Wea. Rev., 114, 824-830.
- \_\_\_\_\_, 1987: Accuracy of multiple-upstream, semi-Lagrangian advective schemes II. Mon. Wea. Rev., 115, 1446-1450.
- \_\_\_\_\_ and J. R. Bates, 1987: Improving the estimate of the departure point position in a two-time level semi-Lagrangian and semi-implicit scheme. Mon. Wea. Rev., 115, 737-739.
- \_\_\_\_\_ and J. R. Bates, 1988: Semi-Lagrangian integration of a grid-point shallow water model on the sphere. Proc. 8th Conference on NWP, Amer. Met. Soc. (to appear).
- McGregor, J. L., 1987: Accuracy and initialization of a two-time-level split semi-Lagrangian model. J. Met. Soc. Japan (in press).
- Phillips, N. A., 1966: The equations of motion for a shallow rotating atmosphere and the "traditional approximation". J. Atmos. Sci., 23, 626-628.
- Ritchie, H., 1986: Eliminating the interpolation associated with the semi-Lagrangian scheme. Mon. Wea. Rev. 114, 135-146.
- \_\_\_\_\_, 1987: Semi-Lagrangian advection on a Gaussian grid. Mon. Wea. Rev., 115, 608-619.
- Robert, A., 1981: A stable numerical integration scheme for the primitive meteorological equations. Atmos.-Ocean, 19, 35-46.
- \_\_\_\_\_, 1982: A semi-Lagrangian and semi-implicit numerical integration scheme for the primitive meteorological equations. J. Met. Soc. Japan, 60, 319-324.
- \_\_\_\_\_, T. L. Yee and H. Ritchie, 1985: A semi-Lagrangian and semi-implicit integration scheme for multi-level atmospheric models. Mon. Wea. Rev., 113, 388-394.

Staniforth, A. N., and C. Temperton, 1986: Semi-implicit semi-Lagrangian integration schemes for a barotropic finite-element regional model. Mon. Wea. Rev., 114, 2078-2090.

Sweet, R. A., 1977: A cyclic reduction algorithm for solving block tridiagonal systems of arbitrary dimension. SIAM J. Numer. Anal., 14, 706-720.

Temperton, C. and A. N. Staniforth, 1987: An efficient two-time-level semi-Lagrangian semi-implicit integration scheme. Quart. J. Roy. Met. Soc., 113, 1025-1039.